

Abstract

We present spectroscopic characterization of 39 early-type stars located in the Kepler satellite field of view. Fourteen stars have been already selected as Kepler targets and they will be observed during the first 9 months of observations. The observations have been carried out at the INAF - Catania Astrophysical Observatory during the summer 2007. For all the stars, using spectral synthesis, we have derived the principal atmospheric parameters such as: effective temperatures, surface gravities and metallicities. Rotational and radial velocities have derived as well. For a few stars also the spectral type has been estimated. Detailed abundances have been computed for the 11 stars with the lowest rotational velocities ($v \sin i \leq 90 \text{ km s}^{-1}$). One of this (HIP 96210) resulted to be a Manganese star. General remarks are discussed in the text.

Characterization of the stellar atmospheres

We have used our spectra to perform the spectral classification of the targets. For this purpose we have degraded their resolution from 20000 to 3000, by convolving them with a Gaussian kernel of the appropriate width, and we have measured the equivalent width of photospheric absorption lines useful for the spectral classification of hot stars, such as: H γ , HeI $\lambda 4471 \text{ \AA}$, and HeI $\lambda 5876 \text{ \AA}$, as well as the MgII $\lambda 4481 \text{ \AA}$ (Hernandez et al., 2004). From their calibration relations EW-Spectral type, we have derived the spectral type. The uncertainty, as derived from the agreement between different diagnostics, is typically of about 1 spectral subclass, but reaches 2 subclasses in the worst cases (lowest S/N and/or high $v \sin i$). The radial velocity measurements were obtained cross-correlating each echelle order of the targets with the corresponding one of a bright RV standard star. We selected: HR1389 (A2IV-V), ι Psc (F7V), and Vega (AOV) as RV standard stars. For this purpose the IRAF task *FXCOR* was used.

The approach we used to determine effective temperature (T_{eff}) and surface gravity ($\log g$) was to compare the observed and theoretical profiles of a Balmer line. In practice, the procedure used for our targets was to minimize the difference among observed and synthetic H β profiles, using as goodness-of-fit parameter the χ^2 . Errors have been estimated as the variation in the parameters which increases the χ^2 of a unit. The synthetic profiles have been computed by using Kurucz codes ATLAS9 and SYNTHE, the former to compute the LTE atmospheric model and the latter to derive the synthetic profiles. The rotational velocity for each star has been computed by matching the observed profile of the MgII $\lambda 4481 \text{ \AA}$ line with a synthetic one. Results are displayed in Tab. 1. For all the slow rotating stars we performed a detailed chemical analysis. We used the atmospheric parameters reported in Tab. 1 to compute the ATLAS9 LTE atmospheric model and SYNTHE to reproduce the observed spectra. Tab. 2 reports the abundances computed for the selected stars. For the remaining fast rotating stars, it was possible only to derive their iron content using two prominent FeII lines, at 5018 \AA and 5316 \AA . The results have been reported in Tab. 3.

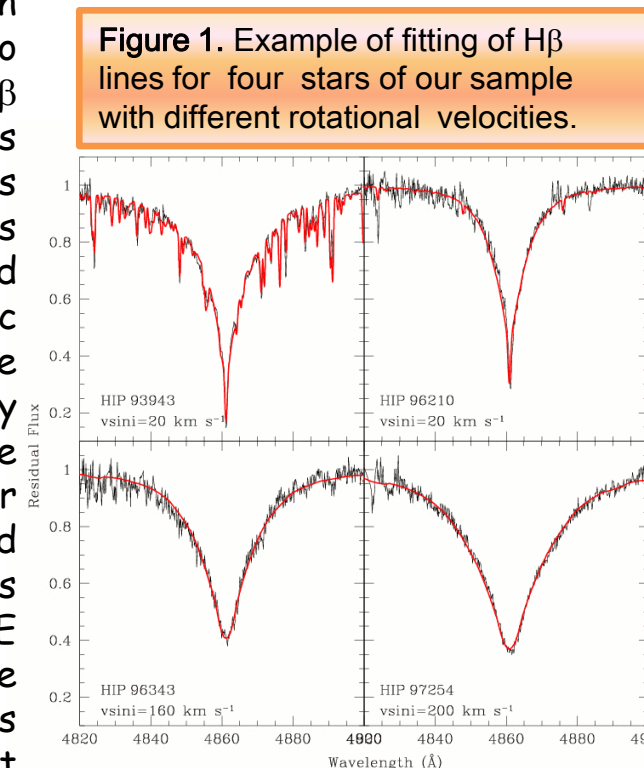


Figure 1. Example of fitting of H β lines for four stars of our sample with different rotational velocities.

Star sample and Observations

Our targets were selected among the 104 Hipparcos stars originally proposed as possible Kepler asteroseismic candidates by Molenda-Żakowicz et al. (2006). All the stars have V magnitudes in the range 9-11 and are among the brightest stars falling in the Kepler field of view. The observations were carried out during the summer 2007 at the M. G. Fracastoro station of the INAF - Catania Astrophysical Observatory with FRESCO, the echelle spectrograph connected by an optical fiber to the 91 cm telescope. The resolving power, as deduced from the calibration lamp lines, was R=21000 and we covered a wavelength range of about 2500 \AA . The signal-to-noise ratio ranges from 30 to 100, depending on the star magnitude and weather conditions. The stellar spectra, calibrated in wavelength and with the continuum normalized to a unity level, were obtained using standard data reduction procedures for spectroscopic observations within the NOAO/IRAF package, that is: bias frame subtraction, trimming, flat-fielding, scattered light correction, fitting traces and orders extraction and, finally, wavelength calibration.

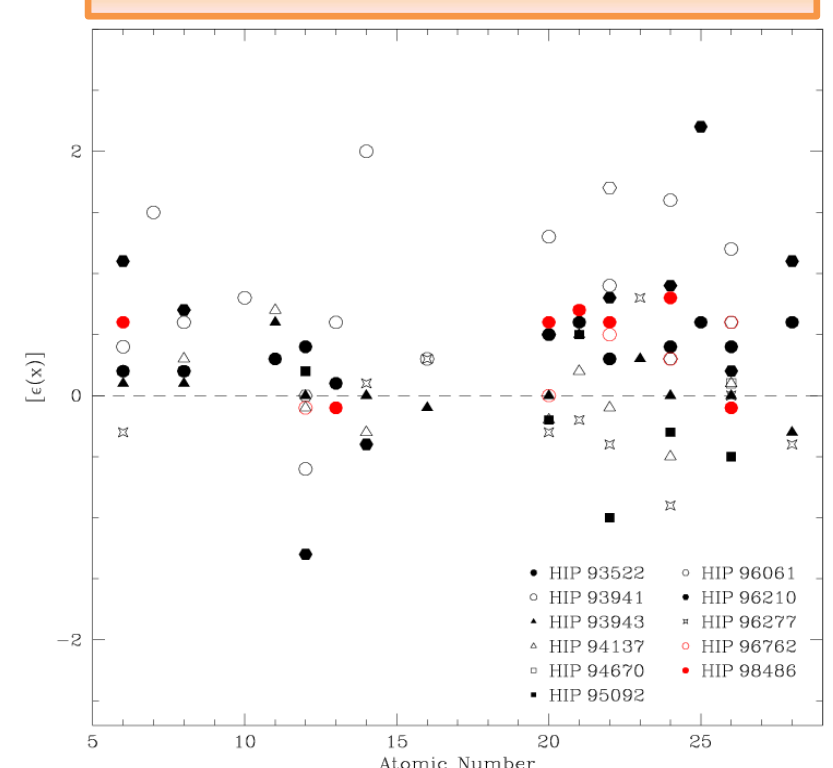
HIP	Other ID	Sp Type	T_{eff} (K)	$\log g$	$v \sin i$ (km s ⁻¹)	HJD (2450000+)	V_{rad} (km s ⁻¹)
91178	HD 172084	A2 \pm 2	9900 \pm 200	4.0 \pm 0.1	110	4306.463	-11.75 \pm 1.38
92247*	BD+48 2768		7200 \pm 200	3.5 \pm 0.2	100	4309.492	-8.26 \pm 2.64
92259	BD+47 2698	A7 \pm 3	7100 \pm 200	3.0 \pm 0.5	120	4310.465	-22.72 \pm 2.58
92637*	BD+48 2781	O9 \pm 2	19900 \pm 1400	3.8 \pm 0.2	230	4307.480	-22.04 \pm 2.80
93070	BD+38 3367		8000 \pm 500	4.2 \pm 0.2	200	4306.580	13.38 \pm 3.21
93522	HD 177484	A7 \pm 2	9100 \pm 400	3.7 \pm 0.2	5	4308.483	1.17 \pm 0.36
93924	HD 178565		10400 \pm 300	4.2 \pm 0.2	150	4306.352	-39.59 \pm 6.51
93941*	BD+42 3250	B2 \pm 2	18700 \pm 4000	3.4 \pm 0.5	10	4270.370	-14.32 \pm 2.98
93943	HD 234806		7400 \pm 200	3.4 \pm 0.5	20	4311.492	-13.63 \pm 0.32
94137	BD+36 3425		7200 \pm 200	4.0 \pm 0.4	50	4311.580	-28.01 \pm 1.23
94670	HD 180757	B9 \pm 2	11600 \pm 500	4.2 \pm 0.2	50	4308.354	-57.17 \pm 1.83
94809	HD 181143		7200 \pm 400	3.9 \pm 0.5	150	4290.393	5.80 \pm 4.44
95069	HD 181879	A1 \pm 2	12300 \pm 700	4.0 \pm 0.2	200	4307.372	-13.81 \pm 1.74
95092	BD+48 2880		8300 \pm 400	3.5 \pm 0.3	80	4307.546	-11.18 \pm 2.13
95174*	HD 182192	A2 \pm 3	10700 \pm 500	4.2 \pm 0.2	200	4306.520	-21.70 \pm 12.1
95495*	BD+49 3002		7000 \pm 200	3.5 \pm 0.5	90	4308.542	-43.94 \pm 1.81
95506	HD 234892	A1 \pm 2	10200 \pm 400	4.0 \pm 0.3	200	4309.345	-22.82 \pm 4.64
96061	BD+52 2452B	B8 \pm 2	12300 \pm 700	4.2 \pm 0.2	70	4285.370	-21.97 \pm 2.21
96210*	BD+41 3394	B6 \pm 2	12600 \pm 600	3.5 \pm 0.3	15	4310.392	6.58 \pm 0.98
96343	HD 234941	B9 \pm 3	11700 \pm 600	4.1 \pm 0.2	160	4311.365	-4.50 \pm 3.13
96762*	HD 185980	B9 \pm 1	10800 \pm 600	4.1 \pm 0.2	10	4309.399	16.51 \pm 1.10
96776	HD 234963		7600 \pm 200	4.5 \pm 0.5	200	4310.541	-7.72 \pm 3.55
97254*	HD 186997	A2 \pm 3	10200 \pm 200	4.2 \pm 0.2	200	4306.403	-4.28 \pm 6.19
97486	TYC 557-1092-1		8000 \pm 300	3.9 \pm 0.4	160	4312.533	-0.81 \pm 4.77
97724*	HD 226221		8900 \pm 400	3.5 \pm 0.2	90	4308.590	-14.76 \pm 4.05
98037*	HD 226571	B6 \pm 2	13100 \pm 700	3.9 \pm 0.2	180	4309.550	-30.9 \pm 20.4
98160*	HD 189159		10000 \pm 300	4.0 \pm 0.2	130	4307.418	-31.72 \pm 5.38
98486	HD 189915		10300 \pm 400	4.0 \pm 0.2	70	4308.409	-23.76 \pm 3.20
96277*	BD+47 2868		7200 \pm 200	3.5 \pm 0.5	60	4278.437	-3.06 \pm 1.77
96277						4313.459	0.71 \pm 1.24
96277						4361.440	-0.78 \pm 1.64
97582*	BD+43 3377		7100 \pm 200	3.6 \pm 0.5	90	4270.494	3.59 \pm 3.46
97582						4361.495	7.10 \pm 6.70
97582						4312.593	2.65 \pm 2.86
98814	V* WW Cyg	B6 \pm 3	13900 \pm 1000	3.9 \pm 0.3	40	4313.372	-40.70 \pm 3.51
96299A*	TYC 3135-651-1				70	4290.556	-7.77 \pm 1.22
96299B						4290.556	45.13 \pm 1.26
98551A	BD+42 3560				70	4313.538	-23.44 \pm 3.29
98551B						4313.538	44.64 \pm 1.97

Table 1. Here we reported: Hipparcos ID, other name, spectral type, T_{eff} , $\log g$, rotational velocity, heliocentric Julian day and radial velocity. All these quantities have been evaluated by us. Stars labelled in red are those for which a detailed abundance analysis have been performed. Footnote a) means that the star has been already selected to be observed with Kepler.

[$\epsilon(X)$]	HIP93522 (9100,3.7)	HIP93941 (18700,3.4)	HIP93943 (7400,3.4)	HIP94137 (7200,4.0)	HIP94670 (11600,4.2)	HIP95092 (8300,3.5)	HIP96061 (12300,4.2)	HIP96210 (12600,3.5)	HIP96277 (7200,3.5)	HIP96762 (10800,4.1)	HIP98486 (10300,4.0)
[C]	0.2 \pm 0.2	0.4 \pm 0.3	0.1 \pm 0.3	0.2 \pm 0.4	---	---	---	1.1 \pm 0.1	-0.3 \pm 0.4	0.6 \pm 0.1	---
[N]	---	1.5 \pm 0.1	---	---	---	---	---	---	---	---	---
[O]	0.2 \pm 0.3	0.6 \pm 0.1	0.1 \pm 0.4	0.3 \pm 0.3	0.2 \pm 0.2	---	---	0.7 \pm 0.2	---	---	---
[Ne]	---	0.8 \pm 0.3	---	---	---	---	---	---	---	---	---
[Na]	0.3 \pm 0.3	---	0.6 \pm 0.5	0.7 \pm 0.3	---	---	---	---	---	---	---
[Mg]	0.4 \pm 0.3	-0.6 \pm 0.1	0.0 \pm 0.2	-0.1 \pm 0.3	0.2 \pm 0.2	0.2 \pm 0.5	0.0 \pm 0.1	-1.3 \pm 0.1	---	---	-0.1 \pm 0.4
[Al]	0.1 \pm 0.1	0.6 \pm 0.4	---	---	---	---	---	0.1 \pm 0.2	-0.1 \pm 0.4	---	---
[Si]	---	2.0 \pm 0.2	0.0 \pm 0.4	-0.3 \pm 0.3	---	---	---	-0.4 \pm 0.1	0.1 \pm 0.4	---	---
[S]	---	0.3 \pm 0.4	-0.1 \pm 0.4	---	---	---	---	0.3 \pm 0.1	---	---	---
[Ca]	0.5 \pm 0.5	1.3 \pm 0.5	0.0 \pm 0.2	-0.2 \pm 0.4	---	-0.2 \pm 0.1	0.5 \pm 0.1	---	-0.3 \pm 0.3	0.6 \pm 0.2	0.0 \pm 0.2
[Sc]	0.6 \pm 0.6	---	0.5 \pm 0.5	0.2 \pm 0.2	---	0.5 \pm 0.2	---	---	-0.2 \pm 0.5	0.7 \pm 0.1	---
[Ti]	0.3 \pm 0.2	0.9 \pm 0.1	0.3 \pm 0.4	-0.1 \pm 0.3	---	-1.0 \pm 0.1	1.7 \pm 0.4	0.8 \pm 0.4	-0.4 \pm 0.2	0.6 \pm 0.3	0.5 \pm 0.1
[V]	---	---	0.3 \pm 0.5	---	---	---	---	0.8 \pm 0.4	---	---	---
[Cr]	0.4 \pm 0.2	1.6 \pm 0.5	0.0 \pm 0.2	-0.5 \pm 0.1	---	-0.3 \pm 0.4	0.3 \pm 0.1	0.9 \pm 0.2	-0.9 \pm 0.2	0.8 \pm 0.4	0.3 \pm 0.1
[Mn]	0.6 \pm 0.4	---	---	---	---	---	---	2.2 \pm 0.2	---	---	---
[Fe]	0.4 \pm 0.1	1.2 \pm 0.4	0.0 \pm 0.1	0.1 \pm 0.3	0.1 \pm 0.3	-0.5 \pm 0.5	0.6 \pm 0.2	0.2 \pm 0.4	0.0 \pm 0.5	-0.1 \pm 0.4	0.6 \pm 0.1
[Ni]	0.6 \pm 0.2	---	-0.3 \pm 0.2	---	---	---	---	1.1 \pm 0.2	-0.4 \pm 0.3	---	---
[Y]	0.0 \pm 0.2	---	0.0 \pm 0.2	0.0 \pm 0.2	---	---	---	0.0 \pm 0.3	---	---	---
[Zr]	---	---	0.0 \pm 0.2	---	---	---	---	---	---	---	---
[Ba]	1.0 \pm 0.3	---	1.0 \pm 0.2	1.0 \pm 0.1	---	---	---	1.0 \pm 0.3	---	---	---

Table 2. Chemical abundances computed for the slow rotating stars ($v \sin i \leq 90 \text{ km s}^{-1}$) of our sample. The abundances are given in terms of the solar ones (Asplund et al., 2005).

Figure 2. Abundance patterns derived for the 11 stars reported in Tab. 2. For the sake of clarity we excluded from the plot all the chemical elements with $Z > 28$.



HIP	[Fe]
91178	0.1
92247	0.4
92259	0.2
93924	0.3
94809	0.4
95174	-0.1
95495	0.4
95506	0.5
96343	0.6
96776	0.7
97254	0.1
97486	0.3
97582	0.2
97724	-0.2
98160	-0.1
98814	0.2

Table 3. Iron abundances for the fast rotating stars of our sample. Typical errors are of the order of 0.2 dex.

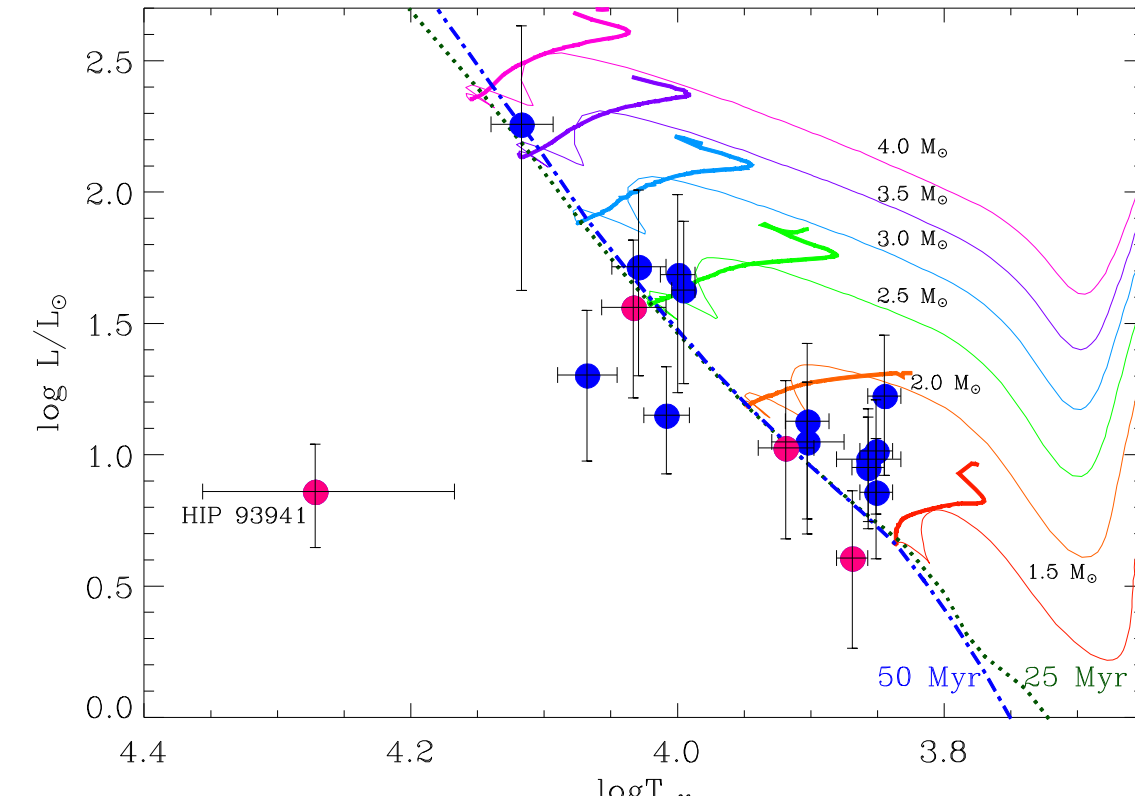


Figure 3. HR diagram of the stars with relative parallax error $\leq 60\%$. Red dots represent the targets for which a detailed abundance analysis has been performed. Evolutionary tracks for stellar masses ranging from 1.5 to 4.0 solar masses have been also displayed (thick lines have been used for the post-main sequence portion of each track). The isochrones at 25 and 50 Myrs are plotted with dotted and dash-dotted lines, respectively (Siess et al., 2000). The star HIP 93941 is really puzzling, because its position on the diagram is not consistent with the derived surface gravity.

Conclusions

In this poster we have presented the preliminary results obtained for a sample of early-type stars candidate to be observed with Kepler satellite. For all the object we computed the radial and rotational velocity, and when possible we estimated the spectral type. Further, we divided our objects in two groups depending to their rotational velocity: slow rotating ($v \sin i \leq 90 \text{ km s}^{-1}$) and fast rotating ($v \sin i > 90 \text{ km s}^{-1}$) stars. For the stars belonging to the former group we undertook a detailed abundance analysis (see Tab. 2), all these stars show more or less standard abundances with the exception of three objects: HIP 93941, HIP 96061 with a enhanced metallicity and HIP 96210 that shows the typical fingerprints of HgMn stars, i.e. strong overabundance (≈ 2.2 dex) of manganese. The stars of the latter group show, instead, standard iron content (see Tab. 3). We have also placed in the HR diagram all the object with a fairly accurate parallax. With the only exception of HIP 93941, they seem to be normal main sequence stars. The former object shows instead a location inconsistent with the stellar parameters determined by us and deserve a more accurate analysis.

References

- Asplund M., Grevesse N., Jacques Sauval A., ASP Conf. Series, Vol. 336, 2005, T. G. Barnes III and F. N. Bash eds
- Hernandez J., Calvet N., Briceno C., Hartmann L., & Berlind P., 2004, AJ, 127, 1682
- Kurucz R. L., IAU colloquium 138, M. M. Dworetsky, F. Castelli and R. Faraggiana eds, ASP Conf. Series Vol. 44, p. 87
- Kurucz R. L., Avrett E. H., 1981, SAO special report 391
- Molenda-Żakowicz, J., Arentoft, T., Kjeldsen, H., & Bonanno, A. 2006, Proc SOHO 18, p.110.1
- Siess L., Dufour E., Forestini M., 2000, A&A, 385, 593